Ursolic acid promotes autophagy by inhibiting Akt/mTOR and TNF-α/TNFR1 signaling pathways to alleviate pyroptosis and necroptosis in Mycobacterium tuberculosis-infected macrophages

Jingjing Shen
Shanghai University of Traditional Chinese Medicine
Yan Fu
Shanghai University of Traditional Chinese Medicine
Fanglin Liu
Shanghai University of Traditional Chinese Medicine
Bangzuo Ning
Shanghai University of Traditional Chinese Medicine
Xin Jiang (jiangxingao@163.com)
Shanghai University of Traditional Chinese Medicine

Research Article

Keywords: Mycobacterium tuberculosis, Pyroptosis, Necroptosis, Autophagy, Ursolic acid, Host-directed therapy

Posted Date: March 29th, 2023

DOI: https://doi.org/10.21203/rs.3.rs-2738766/v1

Additional Declarations: No competing interests reported.

Version of Record: A version of this preprint was published at Inflammation on May 22nd, 2023. See the published version at https://doi.org/10.1007/s10753-023-01839-w.

Abstract

As a lethal infectious disease, tuberculosis (TB) is caused by Mycobacterium tuberculosis (Mtb). Its complex pathophysiological process limits the effectiveness of many clinical treatments. By regulating host cell death, Mtb manipulates macrophages, the first line of defense against invading pathogens, to evade host immunity and promote the spread of bacteria and intracellular inflammatory substances to neighboring cells, resulting in widespread chronic inflammation and persistent lung damage. Autophagy, a metabolic pathway by which cells protect themselves, has been shown to fight intracellular microorganisms, such as Mtb, and they also play a crucial role in regulating cell survival and death. Therefore, host-directed therapy (HDT) based on antimicrobial and anti-inflammatory interventions is a pivotal adjunct to current TB treatment, enhancing anti-TB efficacy. In the present study, we showed that a secondary plant metabolite, ursolic acid (UA), inhibited Mtb-induced pyroptosis and necroptosis of macrophages. In addition, UA induced macrophage autophagy and enhanced intracellular killing of Mtb. To investigate the underlying molecular mechanisms, we explored the signaling pathways associated with autophagy as well as cell death. The results showed that UA could synergistically inhibit the Akt/mTOR and TNF-α/TNFR1 signaling pathways and promote autophagy, thus achieving its regulatory effects on pyroptosis and necroptosis of macrophages. Collectively, UA could be a potential adjuvant drug for host-targeted anti-TB therapy, as it could effectively inhibit pyroptosis and necroptosis of macrophages and counteract the excessive inflammatory response caused by Mtb-infected macrophages via modulating the host immune response, potentially improving clinical outcomes.

1. Introduction

Tuberculosis (TB), caused by Mycobacterium tuberculosis (Mtb) infection, is one of the leading causes of death from infectious agents. Macrophages are the primary host cells of Mtb *in vivo*. After being phagocytosed, Mtb can resist the killing of macrophages and live in macrophages, leading to chronic inflammation and lung damage. The inflammatory response triggered by Mtb infection is a double-edged sword. It is well known that inflammation is a protective host response to infection and tissue damage, preventing pathogen transmission and promoting tissue repair. However, as the inflammatory response develops unbridled, it will become chronic inflammation detrimental to the host [1].

Inflammatory cytokines, such as tumor necrosis factor α (TNF-α) and interleukin-1β (IL-1β), are essential for protecting host cells, while excess cytokine production can lead to increased macrophage death. On the one hand, it will promote the excessive inflammatory reaction of host cells and subsequent severe tissue damage. On the other hand, cell death, cell membrane rupture, and extracellular transmission of Mtb make the infection spread [1]. Therefore, controlling inflammation is an essential approach for effective anti-TB therapy. Host-directed therapy (HDT) is a necessary adjuvant therapy for multidrug-resistant (MDR) TB. HDT can increase the anti-TB efficacy by increasing host immunity, regulating inflammation, reducing lung tissue destruction, and killing or controlling Mtb [2].

Programmed cell death (PCD) is essential for eukaryotic development and integrity, while the dysregulation of this program is associated with many diseases, including immune deficiency, autoimmune diseases, infectious diseases, neurodegenerative diseases, and cancers [3]. Apoptosis is the first known form of cell death, and this immune process is generally silent and noninflammatory. Unlike apoptosis, pyroptosis and necroptosis are lytic forms of cell death that release many intracellular components and immunogenic molecules. Genetic evidence suggests that when these cell death pathways are overactivated, they induce a robust inflammatory response [4-6].

Some studies have shown that pyroptosis and necroptosis in Mtb-infected cells are the main ways of cell death [7]. In previous studies, our group has shown that Mtb infection triggers pyroptosis and expands the inflammatory response [8]. Another process involved in Mtb infection of macrophages, amplifying the inflammatory response, is the inhibition of autophagy. It has been suggested that autophagy induction not only leads to the fusion of the lysosomal compartment with mycobacterial phagosomes but also triggers the production of new antimicrobial peptides, which are essential for mycobacterial killing [9]. Moreover, *in vivo* autophagy experiments have shown that the autophagy protein Atg5 in macrophages is required to inhibit Mtb infection in mice [10], and autophagy inhibitors enhance mycobacterial burden in zebrafish embryonic models [11]. *In vitro* studies have also demonstrated the antibacterial and anti-inflammatory mechanism of autophagy [12]. Besides, our research group has shown that the recovery of autophagy is conducive to the inhibition of pyroptosis. However, the interaction between the autophagy pathway and necroptosis in the pathogenesis of Mtb infection remains largely unexplored.

There is a class of compounds in plants called pentacyclic triterpenes (PT). Ursolic acid (UA) is widely distributed in many plants, fruits, and vegetables [13]. Studies have shown that UA has low cytotoxicity and various pharmacological properties, including anti-tumor, cardioprotective, and hepatoprotective activities, antibacterial and anti-inflammatory properties, and preventive effects of oxidative damage. Furthermore, studies have shown that UA can enhance macrophage autophagy, inhibit IL-1β secretion [14], and reverse TNF-α-induced NLRP3 upregulation [15], suggesting that UA can play an auxiliary anti-inflammatory role in some highly inflammatory diseases. In addition, other studies have shown that UA also plays a vital role in inhibiting bacterial burden and lung inflammation during Mtb infection [16]. However, no studies have focused on the effect of UA on pyroptosis and necroptosis.

In the present study, we also focused on the proinflammatory cytokine TNF-α. TNF-α is closely associated with cell death [17, 18]. TNF-α and tumor necrosis factor receptor-1 (TNFR1) levels were significantly increased in Mtb infected macrophages. Moreover, Akt/mTOR and TNF-α/TNFR1 signal axis occurred upstream of cell death. In conclusion, UA may promote autophagy by inhibiting TNF-α and inhibiting Akt/mTOR pathway, thereby inhibiting pyroptosis and necroptosis. Here, we describe a novel mechanism of UA and demonstrate its anti-inflammatory efficacy as an adjunct anti-tuberculosis agent by inhibiting pyroptosis and necroptosis.

2. Materials and Methods

2.1 Chemicals and Reagents

Dimethyl sulfoxide (DMSO), Phorbol 12-myristate 13-acetate (PMA) were purchased from Sigma (St. Louis, MO). Cell lysis buffer, LDH Cytotoxicity Assay Kit and DAPI were acquired from the Beyotime Institute of Biotechnology (Shanghai, China). Protein A/G Agarose Resin was obtained from Yeasen (Shanghai, China). TNF-α (mouse, 315-01A; human, 300-01A) were purchased from PeproTech. Rapamycin (R8140) and Chloroquine (IC4440) were acquired from Solarbio (Beijing, China). Dulbecco's Modified Eagle's Medium (DMEM) and RPMI 1640 medium were purchased from HyClone Laboratories, Inc (Logan, UT, USA). Middlebrook 7H9 and 7H10 medium were purchased from Difco (Detroit, MI, USA), and oleic acid-albumin-glucose-peroxidase (OADC) supplement was purchased from BD Biosciences (BD, Sparks, MD, USA).

2.2 Cell culture

U937 cell was obtained from ATCC and cultured in RPMI 1640 medium supplemented with 10% fetal bovine serum (FBS), 1% penicillin–streptomycin in 5% CO_2 at 37℃. For differentiation into macrophages, U937 cells were seeded in 6-well plates and treated for 24h with 100 nM PMA. The cells were then replenished with fresh medium immediately before any treatment was used in this study. J774 A.1, a murine macrophage cell line, was obtained from ATCC, and cultured in DMEM supplemented with 10% FBS, 1% penicillin–streptomycin in 5% CO_2 at 37℃.

2.3 Drugs

UA (molecular weight:456.70032, purity >98%, the chemical structure shown in Fig. 1a), a natural pentacyclic triterpenoid carboxylic acid (The full names of the drug have been checked according to http://www.theplantlist.org/), purchased from shanghai Tauto biotech co., LTD. (CAS:77-52-1) (shanghai, China). In the following experiments, we used DMSO to dissolve UA to obtain a 10 μM stock solution, frozen at −20℃, and further diluted to obtain appropriate concentrations (5, 10, or 20 μM) for the experiments.

2.4 Antibodies

Antibodies against GSDMD (A20197), p62 (A11250), Alexa Fluor 488 goat anti-rabbit IgG (AS053) were purchased from ABclonal Technology (Wuhan, China). Antibodies against NLRP3 (15101), Cleaved Caspase-1 (89332), Cleaved Caspase-1 (4199), HMGB1 (3935), RIPK1 (3493), pRIPK1 (Ser166, 53286), pMLKL (Ser345, 34333), LC3B (43566), Akt (4691), p-Akt (4060), mTOR (2972), p-mTOR (5536), Alexa Fluor 594-conjugated goat anti-mouse IgG (8890S) were purchased from Cell Signaling Technology, Inc. (CST, Danvers, MA, USA). Antibodies against pMLKL (Ser358, ab187091), pRIPK3 (Ser232, ab195117), pRIPK3 (Ser227, ab209384) were purchased from Abcam (Cambridge, UK). Antibodies against β-actin (CL594-66009), TNFR1 (21574-1-AP), pRIPK1 (Ser161, 66854-1-Ig) were purchased from ProteinTech Group (Chicago, IL). Antibodies against ASC (SC-514414) was bought from Santa Cruz Biotechnology, Inc.

2.5 Bacterial strains

The Mtb H37Ra was used in this study. H37Ra strain was grown at 37℃ in Middlebrook 7H9 or 7H10 broth supplemented with 0.2% glycerol, 0.05% Tween-80, and 10% Middlebrook OADC supplement.

2.6 Mtb infection

The J774 A.1 or PMA-treated U937 cells were seeded on different cell culture plates and grown at 37℃ overnight. The next day, Mtb H37Ra infected cells for 4 hours when MOI (multiplicity of infection) was 10:1, followed by two PBS washes to remove extracellular bacteria.

2.7 MTT assay

Based on the enzymatic reduction of the water-soluble, yellowish Tetrazolium dye 3-(4,5)-dimethylthiahiazo (-z-y1)-3,5-di-phenytetrazoliumromide (MTT) to purple formazan, is commonly used for assessment of cell viability and proliferation. The J774 A.1 (1×10^4 cells/well) cells or U937 cells (2×10^4 cells/well) were seeded into 96-well plates overnight. The culture medium was substituted with the medium containing different concentrations of UA (0, 2.5, 5, 10, 20, or 40 μM) for 24, 48, and 72 h respectively. After incubation for the assigned period of time, the medium in the wells was discarded. According to the proportion of 100μl containing 10μl MTT (5mg/ml), add to DMEM complete medium mix well, then add to each well and continue to incubate for 4 hours. Whereafter, the medium were aspirated, and the formazan precipitate was dissolved in 150 μl DMSO to lyse the cells. The absorbance was determined at 490 nm employing a Synergy 2 Microplate Reader (Bio-Tek, USA).

2.8 Western blot assay

Total protein was isolated with cell lysis buffer for western blot and Immunoprecipitation (P0013, Beyotime Biotechnology, China). Cells were centrifuged at 12,000 rpm at 4℃ for 15 min and the supernatant was collected. Total protein concentration was evaluated by bicinchoninic acid (BCA) assay (WB6501, NCM Biotech, China). Then, whole cell lysate was added with 5×SDS loading buffer, boiled at 100℃ for 10 min, separated by SDS-PAGE, transferred onto nitrocellulose membranes, blocked in 5% (w/v) skim milk for 1.5 h, incubated with specific primary antibody overnight at 4℃. After three times of washing with TBST, the membranes were incubated with HRP-conjugated secondary antibodies at room temperature for 1h. After extensive washes with TBST, the chemiluminescence was probed by ECL detection kit (Thermo Scientific, MA, USA) with Fluor Chem E (Protein Simple, USA). Band intensities were quantified with the assistance of Image J software (U.S. National Institutes of Health, Bethesda, MD, USA).

2.9 Lactate Dehydrogenase (LDH) Release Assay

Quantification of cytotoxicity can be achieved by examining the activity of LDH released into the culture medium from cells with ruptured plasma membranes. Cells were seeded in 24-well plates and grown at 37°C overnight. Then treated with H37Ra and UA for 24, 48, and 72 h. The cell supernatant was collected

and centrifuged (400g, 5min). Cell death was evaluated applying the LDH Cytotoxicity Assay Kit. Using a microplate reader (490 nm wavelength), the absorbance was determined.

2.10 Coimmunoprecipitation（Co-IP）

J774A.1 and U937 cells were lysed at 4 °C in ice-cold cell lysis buffer, followed by centrifugation at 4 ℃ (12000 rpm, 15 min). Supernatants were collected and incubated with 1–2 μg of the indicated antibody overnight at 4 ℃. Protein A/G agarose beads were added into the lysates and incubated for 3 h at 4 ℃ with gentle rotation. After incubation, the beads were washed 4 times with lysis buffer and boiled in 1×SDS loading buffer at 100℃ for 10 min. Immunoprecipitates in sample buffer were subjected to immunoblotting analysis.

2.11 Immunofluorescence

The cells were seeded in special plates for immunofluorescence, set up control group, Mtb group, Mtb+UA group, and incubated overnight at 37℃. The next day, H37Ra was added after the cells adhered to the wall. After 4 hours of treatment, the cells were washed away with sterile PBS. Fresh medium was added to control group and Mtb group, and fresh drug-containing medium was added to Mtb+UA group. After 12 hours of drug treatment, follow the steps of paraformaldehyde fixation, permeabilization, closure, primary antibody, washing, fluorescent secondary antibody, washing, staining DAPI, washing, and finally adding 1 ml PBS in sequence. The steps after secondary antibody need to be done with care to avoid light. Observe the localization of pMLKL under a confocal microscope. ASC and LC3 co-localization steps are the same as above.

2.12 IL-1β, TNF-α ELISA

After the cells were treated in different ways, the supernatant was collected and centrifuged at 3000rpm for 10min at 4℃. Inflammatory cytokine IL-1β, TNF-α levels were assessed using the IL-1β, TNF-α ELISA kits from R&D System following the manufacturer's protocol.

2.13 Determination of ASC oligomerization

Cells were cultured in 6-well plates overnight, then infected with Mtb and treated with UA 4 hours later. After treated with UA for 12 hours, cells were lysed with Triton Buffer (PBS, 0.5% Triton X-100) and then centrifuged at 6000g at 4℃ for 15 minutes. The pellets were washed with PBS, and then cross-linked by incubation with 2 mM disuccinimidyl suberate (DSS, Sigma-Aldrich) for 30 min at room temperature. Subsequently, the sample was centrifuged again at 6000g for 15 min at 4 ℃. The supernatants were discarded, and 40 μl of 1× SDS loading buffer was added to crosslinked pellets. The samples were boiled at 100 ℃ for 10 min and then subjected to separation through SDS-PAGE.

2.14 Statistical analysis

Statistical analyses were performed using GraphPad Prism 9 (GraphPad Software, La Jolla, CA, USA). Statistical significance was analyzed by one-way ANOVA analysis, and the results were expressed as mean ± standard deviation (SD). The data showed are representative of at least three repeated experiments. $p < 0.05$ was considered statistically significant.

3. Results

3.1 Effect of UA on the viability of J774A.1 and U937 cells

In order to select the appropriate drug concentration for subsequent experiments, the cytotoxicity of UA was determined by MTT assay. Using three time points (24, 48, and 72 h), we found that UA did not affect the viability of J774A.1 and U937 cells at a dose of 10 μM (Fig. 1b, 1c). Therefore, the concentration of UA within 10 μM was considered safe and adopted for subsequent experiments.

3.2 UA inhibits cell death induced by Mtb infection

To examine Mtb-induced cell death *in vitro*, we employed a model in which J774A.1 or U937 cells were exposed to Mtb, and cell death was evaluated by detecting the release of lactate dehydrogenase (LDH). As a stable enzyme in all cell types, LDH is rapidly released into the cell culture medium after cell death and plasma membrane damage. Therefore, LDH is a critical marker used in cell death studies. The results demonstrated that the proportion of LDH released by macrophages increased after Mtb infection, which was rescued by UA treatment (Fig. 2a, 2b). Furthermore, the change in LDH activity indicated that UA could alter the plasma membrane permeability of J774A.1 and U937 cells.

3.3 UA alleviates pyroptosis in Mtb-infected macrophages

Pyroptosis, also known as inflammatory cell necrosis, is a violently programmed cell lysis of death [19]. The inflammasome activation plays a primary role in the occurrence and development of pyroptosis. For example, the NOD-like receptor (NLR) family member NLRP3 assembles intracellular protein complexes called NLRP3 inflammasomes in response to sensing certain pathogen products or sterile danger signals, which is a well-studied inflammasome [20, 21].

Our previous studies have proved that Mtb-infected macrophages can promote the activation of the NLRP3 inflammasome, thereby causing pyroptosis and leading to the spread of bacteria and a severe inflammatory reaction [8, 12, 22]. In the present study, we found that UA significantly inhibited the expression of NLRP3 in a time- and concentration-dependent manner (Fig. 3a-3d) and inhibited the formation of Apoptosis-associated speck-like protein containing a caspase recruitment domain (ASC) oligomerization (Fig. 3e, 3f), thereby inhibiting the assembly of the NLRP3 inflammasome (Fig. 3g, 3h), effectively suppressing the activity of caspase-1, blocking N-terminal fragment of GSDMD (GSDMD-N), and inhibiting the occurrence of pyroptosis (Fig. 3i, 3j). In addition, UA inhibited the expression of High-mobility group box 1 protein (HMGB1) (Fig. 3i, 3j), which is closely related to inflammatory response, and

suppressed the secretion of inflammatory factor IL-1β in a concentration-dependent manner (Fig. 3k, 3l), thus restricting the excessive inflammatory response.

3.4 UA alleviates necroptosis in Mtb-infected macrophages

Necroptosis is another form of inflammatory cell death triggered by extracellular stimuli that activate inflammation and cell death. Necroptosis is induced by various signals, including cell death receptor ligands, among which the TNF-α/TNFR1 signaling pathway is the most representative [23]. We demonstrated that during Mtb infection, TNF-α was overcharged, and UA inhibited the release of TNF-α (Fig. 4a, 4c) and the overactivation of TNFR1 (Fig. 4b, 4d). In the necroptosis pathway, the RIPK1-RIPK3-MLKL signaling cascade is a crucial feature. Sequential phosphorylation of receptor-interacting protein kinase 1 (RIPK1) and RIPK3, which in turn phosphorylates pseudokinase mixed lineage kinase domain-like (MLKL) protein. This process leads to MLKL oligomerization and translocation to the plasma membrane, disrupting cell membrane integrity, and resulting in lytic cell death [24]. Our data supported that RIPK1, RIPK3, and MLKL were phosphorylated after Mtb infection, and the phosphorylation degree of these proteins was decreased after UA treatment (Fig. 4e, 4f). Correspondingly, the immunofluorescence assay showed that UA inhibited the accumulation of phosphorylated MLKL (pMLKL) on the cell membrane after Mtb infection (Fig. 4g, 4h).

3.5 UA induces autophagy in macrophages by inhibiting the Akt/mTOR pathway

Autophagy plays a vital role in both innate and adaptive immunities of the host infected with Mtb, which is reflected in the degradation of dysfunctional and unnecessary cellular components in the process of autophagy to achieve cell homeostasis and organelle renewal [25].

The ability of Mtb to survive and replicate in host macrophages is the core of the TB mechanism [9, 26]. Some studies have demonstrated that Mtb clearance can be enhanced by targeting the macrophage autophagy mechanism to reduce inflammation [12, 27]. To evaluate the ability of UA to induce autophagy in Mtb infection, we measured the expressions of p62 and LC3 II at the protein level when exposed to different concentrations of UA (0, 5, 10, or 20 μM) and at different times of treatment. P62 is a selective substrate for autophagy and a marker of autophagy flux. LC3 lipidation is a specific marker of autophagosome in mammalian cells, widely used in autophagy detection. Our results showed that UA treatment decreased the expression of p62 and increased the expression of LC3 II in a concentration- and time-dependent manner (Fig. 5a-5d).

Many studies have reported that Akt/mTOR is a classical negative regulator of autophagy [28, 29]. Western blot analysis showed that Mtb treatment significantly enhanced the expressions of phosphorylated Akt (p-Akt) and phosphorylated mTOR (p-mTOR) at the protein level compared with the control group. However, UA treatment down-regulated the elevation of p-Akt and p-mTOR in a time-dependent manner (Fig. 5e, 5f). Based on these results, we concluded that UA could inhibit Akt/mTOR signaling pathway to activate autophagy.

3.6 UA inhibits pyroptosis and necroptosis by promoting autophagy

Some studies have shown that the activation of autophagy can inhibit pyroptosis [30-32], and autophagy can also regulate necroptosis [33, 34]. Based on the above results, we proposed a conjecture as follows: is there any relationship between autophagy, pyroptosis, and necroptosis in Mtb-infected macrophages? Therefore, in the present study, we adopted the classical activator of autophagy rapamycin (Rapa) and the autophagy inhibitor chloroquine (CQ) to investigate the effects of autophagy on pyroptosis and necroptosis of J774A.1 and U937 cells. The expressions of p62, LC3 II, GSDMD-N, and pMLKL were detected by Western blot analysis after treatment with Rapa, CQ, and UA.

On the one hand, similar to Rapa treatment, UA treatment also inhibited the expression of p62 and enhanced the expression of LC3 II, indicating that UA had a brilliant ability to promote autophagy. After treatment with Rapa and UA, the expressions of GSDMD-N, an essential protein of pyroptosis, and pMLKL, a key protein of necroptosis, were decreased. On the other hand, the results were further verified by CQ. The results showed that 20 μM CQ caused significant accumulation of p62 and LC3 II, increased the expressions of GSDMD-N and pMLKL, and blocked the smooth autophagy flow process induced by UA and the inhibition of pyroptosis and necroptosis to a certain extent (Fig. 6a, 6b).

Furthermore, we observed that UA could promote the co-localization of ASC and LC3 through confocal microscopy (Fig. 6c, 6d), which further verified the close connection between autophagy and pyroptosis. In addition, it has been noted in the literature that the ZZ domain of p62 (amino acid 122-167) interacts with RIPK1 [33, 35], which was also confirmed by Co-IP, and UA inhibited the interaction of p62 with RIPK1 compared with the Mtb group (Fig. 6e, 6f). RIPK1, a member of the death domain family of proteins, acts as a primary upstream regulator that controls cell survival and inflammatory signaling, including necroptosis [36]. Therefore, the inhibition of the interaction between p62 and RIPK1 by UA also indirectly indicated the close relationship between autophagy and necroptosis. In conclusion, UA inhibited pyroptosis and necroptosis by promoting autophagy.

3.7 UA promotes autophagy and inhibits pyroptosis and necroptosis, which is related to TNF-α/TNFR1.

As mentioned above, TNF-α overproduction promotes the progression of TB and is not conducive to host recovery, and TNF-α plays a crucial role in mediating the occurrence and development of necroptosis and pyroptosis [18, 23, 37]. TNF-α has also been reported to be associated with autophagy [38]. Therefore, we tried to investigate the role of TNF-α in necroptosis, pyroptosis, and autophagy. We detected the expressions of related indicators by exposing the Mtb-infection macrophages to a specific dose of TNF-α. As expected, we found that pMLKL and GSDMD-N were significantly up-regulated after co-incubation with TNF-α compared with the Mtb group, and UA could still inhibit the enhanced expressions of pMLKL and GSDMD-N after TNF-α treatment. In addition, it was worth noting that autophagy also showed a correlation with TNF-α. Compared with the Mtb group, the addition of TNF-α resulted in a significant accumulation of p62 and LC3 proteins, inhibiting autophagy and impeding UA-induced patency of the autophagic flow process (Fig. 7a, 7b).

4. Discussion

TB remains the leading cause of infectious death worldwide. Current research has found that the primary cause of death in most people infected with Mtb in the fight against TB is severe tissue damage due to the excessive inflammation that results from the infection. Mtb has evolved immune evasion mechanisms that bypass the macrophage-killing mechanism by blocking phagosome maturation, mediating inflammation, and manipulating the host cell death program through a series of proteins encoded by its virulence genes [39]. The inflammatory response induced by Mtb infection is a double-edged sword. The excessive inflammatory response promotes cell death, cell membrane rupture, and intracellular diffusion, allowing for the amplification of the infection [1]. Therefore, treatment of excessive inflammation induced by Mtb infection can help advance the treatment process. HDT is based on balancing the host immune system and may provide a new avenue for discovering new anti-TB therapies.

In recent years, PCD does not only refer to apoptosis with the discovery of various cell death forms, such as pyroptosis and necroptosis. Different forms of cell death have various impacts on the body due to their different mechanisms [40]. Pyroptosis and necroptosis are lytic forms of cell death that release potentially immune stimulatory molecules and have been described as proinflammatory cell death [6]. The inflammasome activation plays a vital role in the classical pyroptosis pathway. Necroptosis, another form of inflammatory PCD, is often seen as a backup defense mechanism against cell death. Triggered when apoptotic caspase-8 is impeded, TNF-α binding to TNFR1 is the most characteristic triggering condition of necroptosis *in vitro* [41].

UA belongs to terpenoids and is widely distributed in natural plants. Previous studies have shown that UA can play an auxiliary anti-inflammatory role in some highly inflammatory diseases [15]. Our results showed that UA inhibited the activation of the NLRP3 inflammasome, the cleavage of caspase-1 and GSDMD, and the release of IL-1β. In addition, UA inhibited TNF-α/TNFR1 and suppressed the cascade activation of RIPK1-RIPK3-MLKL. Therefore, pyroptosis and necroptosis co-existed in the process of Mtb infection, which expanded the inflammatory response. However, to our knowledge, we showed UA's effects on pyroptosis and necroptosis for the first time.

Since UA inhibited the expressions of crucial molecules involved in pyroptosis and necroptosis, we further explored whether there were relevant regulatory mechanisms upstream to manipulate these changes. Autophagy widely exists in eukaryotic cells as a self-protection mechanism and is akin to a self-feeding phenomenon. Autophagy leads to the lysosomal degradation of damaged organelles, old and abnormal or non-functional proteins, and other substances in the cell; implementation of cellular energy metabolism, maintenance of cellular homeostasis, and regulation of cell survival and death [42]. Previously, our group has demonstrated that activation of the Akt/mTOR signaling pathway during Mtb infection leads to the inhibition of autophagy and ultimately exacerbates the inflammatory response [12]. We demonstrated that UA activated autophagy by inhibiting the classical autophagy signaling pathway Akt/mTOR and maintaining cell homeostasis.

However, then the question arises. Is there a parallel relationship between the activation of autophagy by UA and the inhibition of pyroptosis and necroptosis? Or is there some concatenation? Studies have shown that in the absence of Dram1, a stress-induced regulator of autophagy, infected macrophages become overburdened with bacteria, initiating pyroptosis and leading to the spread of infection [43]. This finding suggests that inhibition of autophagy promotes the activation of pyroptosis in Mtb infection models. Although no studies have pointed to a relationship between autophagy and necroptosis in Mtb infection models, it shows that autophagy can regulate necroptosis in other infection models [33]. Therefore, we hypothesized a similar association between autophagy and necroptosis in this study model, and UA might reverse inflammatory cell death by promoting autophagy. By adopting the autophagy activator Rapa and the autophagy inhibitor CQ, we proved that UA reversed pyroptosis and necroptosis by promoting autophagy.

Moving on to the details of the inferred pathway, RIPK1 is a crucial scaffold protein that regulates cell death and inflammation. RIPK1 has been implicated downstream of various immune receptors [44, 45], and most studies have focused on TNF-α/TNFR1-mediated RIPK1 activation. We found that the RIPK1/RIPK3/MKL cascade was activated in Mtb-infected macrophages. We focused on p62, which is not only involved in autophagy but also a RIPK1 binding protein [33, 35]. In our cell culture model, we verified the formation of the p62-RIPK1 complex, which was inhibited by UA treatment. The inhibition of autophagy substrate p62 by UA could be interpreted as the degradation of p62 due to the activation of autophagy by UA. Therefore, the binding of p62 and RIPK1 was reduced accordingly. This finding also indirectly further illustrated the regulation of necroptosis by autophagy.

In addition, combined with the detrimental effect of cytokine overproduction on the development of inflammation and the significant inhibitory effect of UA on the expressions of TNF-α and its receptor TNFR1 after Mtb infection, we also focused on the critical proinflammatory factor TNF-α, which is closely associated with the process of Mtb infection. It has been suggested that TNF-α is closely associated with necroptosis and pyroptosis [38]. In addition, TNF-α inducing necroptosis inhibits late autophagy [46]. Our results were consistent with the findings mentioned above. Mtb successfully escaped autophagy and induced necroptosis and pyroptosis. UA could reverse this event, which was primarily related to the inhibition of TNFα/TNFR1 by UA.

In summary, our data indicated that UA had an antibacterial and anti-inflammatory effect on Mtb-infected macrophages, which was reflected by the effect of UA on several key continuous events, namely, inhibition of Akt/mTOR signaling pathway, induction of autophagy flux activation, inhibition of pyroptosis and necroptosis, and maintenance of cell homeostasis (Fig. 8). These results suggested that UA could be used as a novel HDT candidate for adjuvant therapy against TB to reduce the side effects of antibiotics and enhance efficacy. In addition, this study on the inflammatory cell death caused by Mtb infection of macrophages provided more perspectives for further understanding of the pathophysiology and escape mechanism of Mtb, which might provide some references for finding more critical and practical targets in the next step.

In the present study, we used the *in vitro* infection model of H37Ra, which is an attenuated strain and evolved from H37 like its sister strain H37Rv [47]. Although there are differentially expressed genes in the two strains, H37Ra is considered a good material for studying virulence genes and the pathogenic mechanism of Mtb because it retains the immunogenicity of the strains and has particular safety. Therefore, elucidating the pathogenic mechanism of H37Ra is of great significance for understanding the pathogenic mechanism of Mtb [48]. In addition, future studies are needed to further focus on the combination of UA with first-line anti-TB drugs to improve the treatment of TB in animal models and clarify whether there is potential for clinical application.

Declarations

Acknowledgements

The authors thank all the members of the laboratory for their help.

Availability of data and materials

The data used to support the findings of this study are available from the corresponding author upon request.

Competing Interests

The authors declare no competing interests.

Author Contributions

XJ conceived and designed the experiments. JS, YF, FL, and BN performed the experiments. JS and YF analyzed the data. JS and XJ wrote the paper. All authors have read and approved the final manuscript.

Consent for publication

Not applicable.

Funding

This study was supported by National Key Research and Development Program of China (2021YFE0200900), National Natural Science Foundation of China (81873069) Shanghai Municipal Science and Technology Major Project (ZD2021CY001).

References

1. Ravesloot-Chavez, M.M., E. Van Dis, and S.A. Stanley, The Innate Immune Response to Mycobacterium tuberculosis Infection. *Annu Rev Immunol*, 2021. **39**: p. 611-637.

2. Tiberi, S., et al., Tuberculosis: progress and advances in development of new drugs, treatment regimens, and host-directed therapies. *Lancet Infect Dis*, 2018. **18**(7): p. e183-e198.
3. Ameisen, J.C., On the origin, evolution, and nature of programmed cell death: a timeline of four billion years. *Cell Death Differ*, 2002. **9**(4): p. 367-93.
4. Liu, X. and J. Lieberman, A Mechanistic Understanding of Pyroptosis: The Fiery Death Triggered by Invasive Infection. *Adv Immunol*, 2017. **135**: p. 81-117.
5. Weinlich, R., et al., Necroptosis in development, inflammation and disease. *Nat Rev Mol Cell Biol*, 2017. **18**(2): p. 127-136.
6. Frank, D. and J.E. Vince, Pyroptosis versus necroptosis: similarities, differences, and crosstalk. *Cell Death Differ*, 2019. **26**(1): p. 99-114.
7. Beckwith, K.S., et al., Plasma membrane damage causes NLRP3 activation and pyroptosis during Mycobacterium tuberculosis infection. *Nat Commun*, 2020. **11**(1): p. 2270.
8. Li, Y., et al., Tanshinone IIA alleviates NLRP3 inflammasome-mediated pyroptosis in Mycobacterium tuberculosis-(H37Ra-) infected macrophages by inhibiting endoplasmic reticulum stress. *J Ethnopharmacol*, 2022. **282**: p. 114595.
9. Espert, L., B. Beaumelle, and I. Vergne, Autophagy in Mycobacterium tuberculosis and HIV infections. *Front Cell Infect Microbiol*, 2015. **5**: p. 49.
10. Castillo, E.F., et al., Autophagy protects against active tuberculosis by suppressing bacterial burden and inflammation. *Proc Natl Acad Sci U S A*, 2012. **109**(46): p. E3168-76.
11. van der Vaart, M., et al., The DNA damage-regulated autophagy modulator DRAM1 links mycobacterial recognition via TLR-MYD88 to autophagic defense [corrected]. *Cell Host Microbe*, 2014. **15**(6): p. 753-67.
12. Zhang, Q., et al., Antimycobacterial and Anti-inflammatory Mechanisms of Baicalin via Induced Autophagy in Macrophages Infected with Mycobacterium tuberculosis. *Front Microbiol*, 2017. **8**: p. 2142.
13. Mlala, S., et al., Ursolic Acid and Its Derivatives as Bioactive Agents. *Molecules*, 2019. **24**(15).
14. Leng, S., et al., Ursolic acid enhances macrophage autophagy and attenuates atherogenesis. *J Lipid Res*, 2016. **57**(6): p. 1006-16.
15. Wang, C., et al., Ursolic acid protects chondrocytes, exhibits anti-inflammatory properties via regulation of the NF-kappaB/NLRP3 inflammasome pathway and ameliorates osteoarthritis. *Biomed Pharmacother*, 2020. **130**: p. 110568.
16. Jimenez-Arellanes, A., et al., Ursolic and oleanolic acids as antimicrobial and immunomodulatory compounds for tuberculosis treatment. *BMC Complement Altern Med*, 2013. **13**: p. 258.
17. Chen, A.Q., et al., Microglia-derived TNF-alpha mediates endothelial necroptosis aggravating blood brain-barrier disruption after ischemic stroke. *Cell Death Dis*, 2019. **10**(7): p. 487.
18. Wang, Y., et al., TNF-alpha/HMGB1 inflammation signalling pathway regulates pyroptosis during liver failure and acute kidney injury. *Cell Prolif*, 2020. **53**(6): p. e12829.

19. Rao, Z., et al., Pyroptosis in inflammatory diseases and cancer. *Theranostics*, 2022. **12**(9): p. 4310-4329.
20. Liang, F., et al., The advances in pyroptosis initiated by inflammasome in inflammatory and immune diseases. Inflamm Res, 2020. **69**(2): p. 159-166.
21. Kesavardhana, S. and T.D. Kanneganti, Mechanisms governing inflammasome activation, assembly and pyroptosis induction. *Int Immunol*, 2017. **29**(5): p. 201-210.
22. Fu, Y., et al., Andrographolide Suppresses Pyroptosis in Mycobacterium tuberculosis-Infected Macrophages via the microRNA-155/Nrf2 Axis. *Oxid Med Cell Longev*, 2022. **2022**: p. 1885066.
23. Choi, M.E., et al., Necroptosis: a crucial pathogenic mediator of human disease. *JCI Insight*, 2019. **4**(15).
24. Zhang, Y., et al., Plasma membrane changes during programmed cell deaths. *Cell Res*, 2018. **28**(1): p. 9-21.
25. Lam, A., et al., Role of apoptosis and autophagy in tuberculosis. *Am J Physiol Lung Cell Mol Physiol*, 2017. **313**(2): p. L218-L229.
26. Weiss, G. and U.E. Schaible, Macrophage defense mechanisms against intracellular bacteria. *Immunol Rev*, 2015. **264**(1): p. 182-203.
27. Chai, Q., et al., New insights into the evasion of host innate immunity by Mycobacterium tuberculosis. Cell Mol Immunol, 2020. **17**(9): p. 901-913.
28. Sun, K., et al., The PI3K/AKT/mTOR signaling pathway in osteoarthritis: a narrative review. *Osteoarthritis Cartilage*, 2020. **28**(4): p. 400-409.
29. Liu, B., et al., Scoparone improves hepatic inflammation and autophagy in mice with nonalcoholic steatohepatitis by regulating the ROS/P38/Nrf2 axis and PI3K/AKT/mTOR pathway in macrophages. *Biomed Pharmacother*, 2020. **125**: p. 109895.
30. Li, M.Y., et al., Adrenomedullin alleviates the pyroptosis of Leydig cells by promoting autophagy via the ROS-AMPK-mTOR axis. *Cell Death Dis*, 2019. **10**(7): p. 489.
31. Meng, Q., et al., Estrogen prevent atherosclerosis by attenuating endothelial cell pyroptosis via activation of estrogen receptor alpha-mediated autophagy. *J Adv Res*, 2021. **28**: p. 149-164.
32. Wu, C., et al., Betulinic acid inhibits pyroptosis in spinal cord injury by augmenting autophagy via the AMPK-mTOR-TFEB signaling pathway. *Int J Biol Sci*, 2021. **17**(4): p. 1138-1152.
33. Xu, C., et al., TNF-alpha-dependent neuronal necroptosis regulated in Alzheimer's disease by coordination of RIPK1-p62 complex with autophagic UVRAG. *Theranostics*, 2021. **11**(19): p. 9452-9469.
34. Matsuzawa-Ishimoto, Y., et al., Autophagy protein ATG16L1 prevents necroptosis in the intestinal epithelium. *J Exp Med*, 2017. **214**(12): p. 3687-3705.
35. Sanz, L., et al., The interaction of p62 with RIP links the atypical PKCs to NF-kappaB activation. *EMBO J*, 1999. **18**(11): p. 3044-53.

36. Xu, D., C. Zou, and J. Yuan, Genetic Regulation of RIPK1 and Necroptosis. *Annu Rev Genet*, 2021. **55**: p. 235-263.
37. Yao, F., et al., HDAC11 promotes both NLRP3/caspase-1/GSDMD and caspase-3/GSDME pathways causing pyroptosis via ERG in vascular endothelial cells. *Cell Death Discov*, 2022. **8**(1): p. 112.
38. Ezquerro, S., et al., Ghrelin Reduces TNF-alpha-Induced Human Hepatocyte Apoptosis, Autophagy, and Pyroptosis: Role in Obesity-Associated NAFLD. *J Clin Endocrinol Metab*, 2019. **104**(1): p. 21-37.
39. Hmama, Z., et al., Immunoevasion and immunosuppression of the macrophage by Mycobacterium tuberculosis. *Immunol Rev*, 2015. **264**(1): p. 220-32.
40. Lee, K.H. and T.B. Kang, The Molecular Links between Cell Death and Inflammasome. *Cells*, 2019. **8**(9).
41. D'Arcy, M.S., Cell death: a review of the major forms of apoptosis, necrosis and autophagy. *Cell Biol Int*, 2019. **43**(6): p. 582-592.
42. Zhao, J., et al., Apoptosis, Autophagy, NETosis, Necroptosis, and Pyroptosis Mediated Programmed Cell Death as Targets for Innovative Therapy in Rheumatoid Arthritis. *Front Immunol*, 2021. **12**: p. 809806.
43. Zhang, R., et al., Deficiency in the autophagy modulator Dram1 exacerbates pyroptotic cell death of Mycobacteria-infected macrophages. *Cell Death Dis*, 2020. **11**(4): p. 277.
44. Jouan-Lanhouet, S., et al., Necroptosis, in vivo detection in experimental disease models. *Semin Cell Dev Biol*, 2014. **35**: p. 2-13.
45. Riebeling, T., et al., Primidone blocks RIPK1-driven cell death and inflammation. *Cell Death Differ*, 2021. **28**(5): p. 1610-1626.
46. Wu, W., et al., TNF-induced necroptosis initiates early autophagy events via RIPK3-dependent AMPK activation, but inhibits late autophagy. *Autophagy*, 2021. **17**(12): p. 3992-4009.
47. Palendira, U., et al., Lymphocyte recruitment and protective efficacy against pulmonary mycobacterial infection are independent of the route of prior Mycobacterium bovis BCG immunization. *Infect Immun*, 2002. **70**(3): p. 1410-6.
48. Zheng, H., et al., Genetic basis of virulence attenuation revealed by comparative genomic analysis of Mycobacterium tuberculosis strain H37Ra versus H37Rv. *PLoS One*, 2008. **3**(6): p. e2375.

Figures

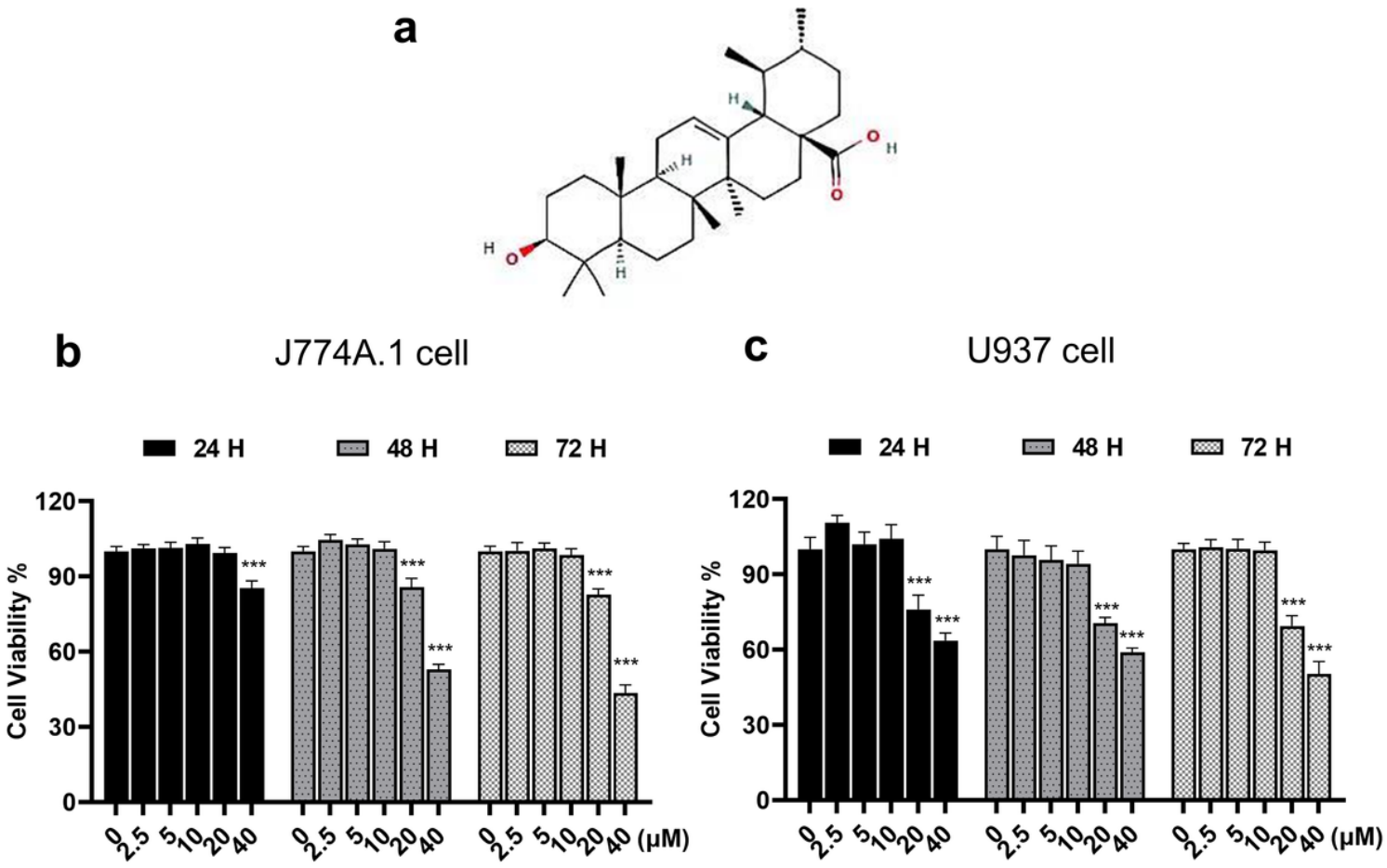

Figure 1

Effect of UA on the viability of J774A.1 and U937 cells. **a** The chemical structure of UA. **b** Proliferation assay to assess the cytotoxic effect of UA on J774A.1 cell. **c** Proliferation assay to assess the cytotoxic effect of UA on U937 cell. Data are shown as mean ± SD of at least three independent experiments. $***p < 0.001$.

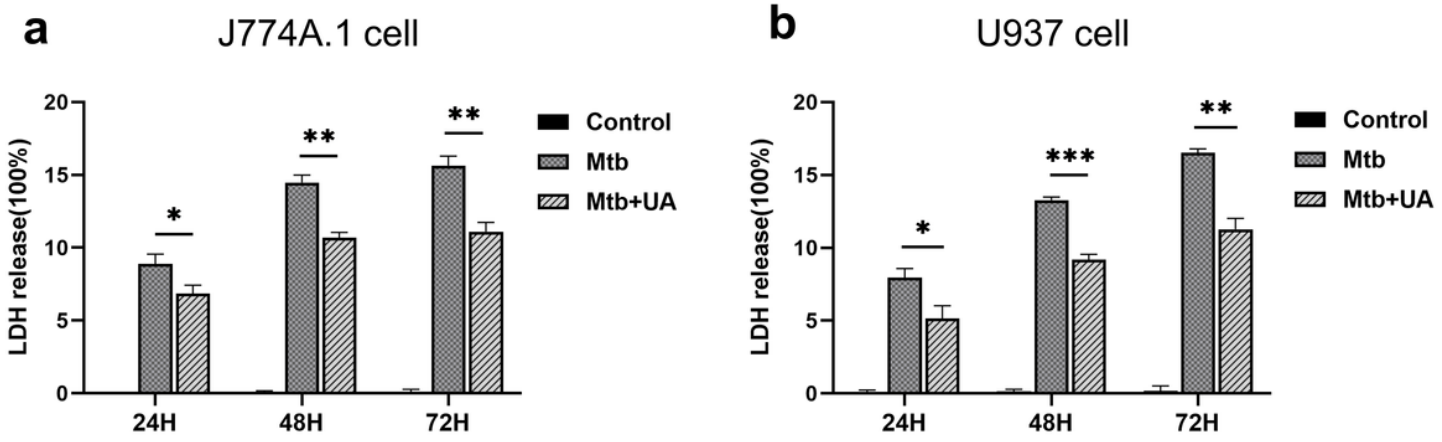

Figure 2

UA inhibits cell death induced by Mtb infection. **a, b** The levels of LDH released from the supernatants of J774A.1 and U937 cells were measured using LDH Cytotoxicity Assay kit, respectively. Data are shown as mean ± SD of three independent experiments. $*p < 0.05$, $**p < 0.01$, and $***p < 0.001$.

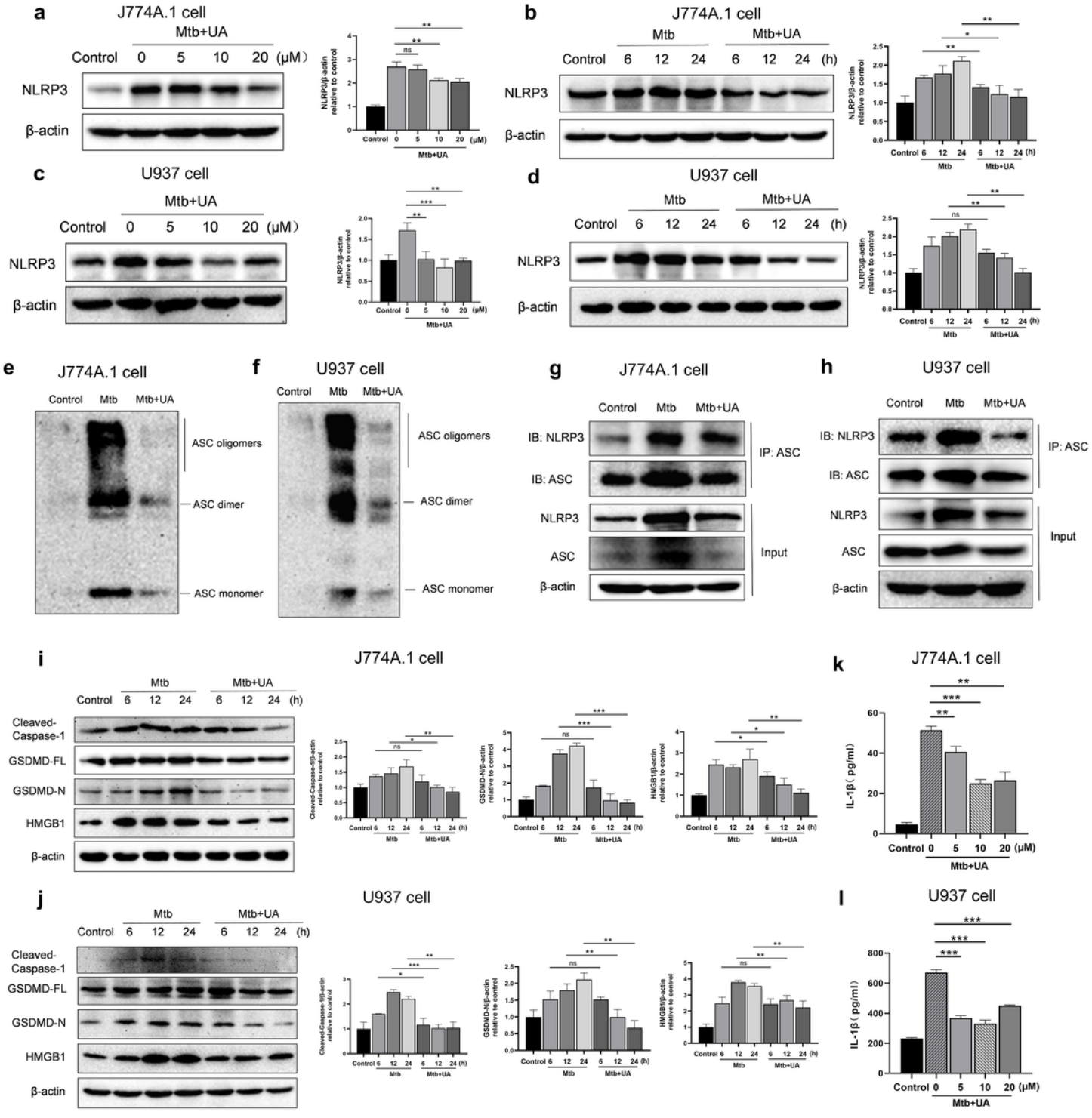

Figure 3

UA alleviates pyroptosis in Mtb-infected macrophages. **a-d** The protein expression levels of NLRP3 in cell lysates of J774A.1 and U937 cells were determined by western blot assay, respectively. The bar graph

below shows the statistical results of the grayscale values of NLRP3 protein levels. **e, f** Protein fractions of different treatment groups and DSS cross-linked in J774A.1 and U937 cells were analyzed by western blot, respectively, as indicated. The monomer, dimer, and oligomers forms of ASC are indicated in the figures. **g, h** The effect of UA on ASC and NLRP3 protein interactions was examined in J774A.1 and U937 cells that have been validated to express ASC and NLRP3, after Mtb treatment alone or in combination with UA, and immunoprecipitated with anti-ASC antibody. **i, j** The effects of UA on the expression of pyroptosis-associated proteins Cleaved-Caspase-1, GSDMD-N and HMGB1 in J774A.1 and U937 cells were detected by western blot, and the results of grayscale values were counted. **k, l** The inhibition of Mtb-induced IL-1β content in J774A.1 and U937 cells by different concentrations of UA were detected by ELISA. Data are shown as mean ± SD of three independent experiments. $*p < 0.05$, $**p < 0.01$, and $***p < 0.001$. ns: nonsignificant.

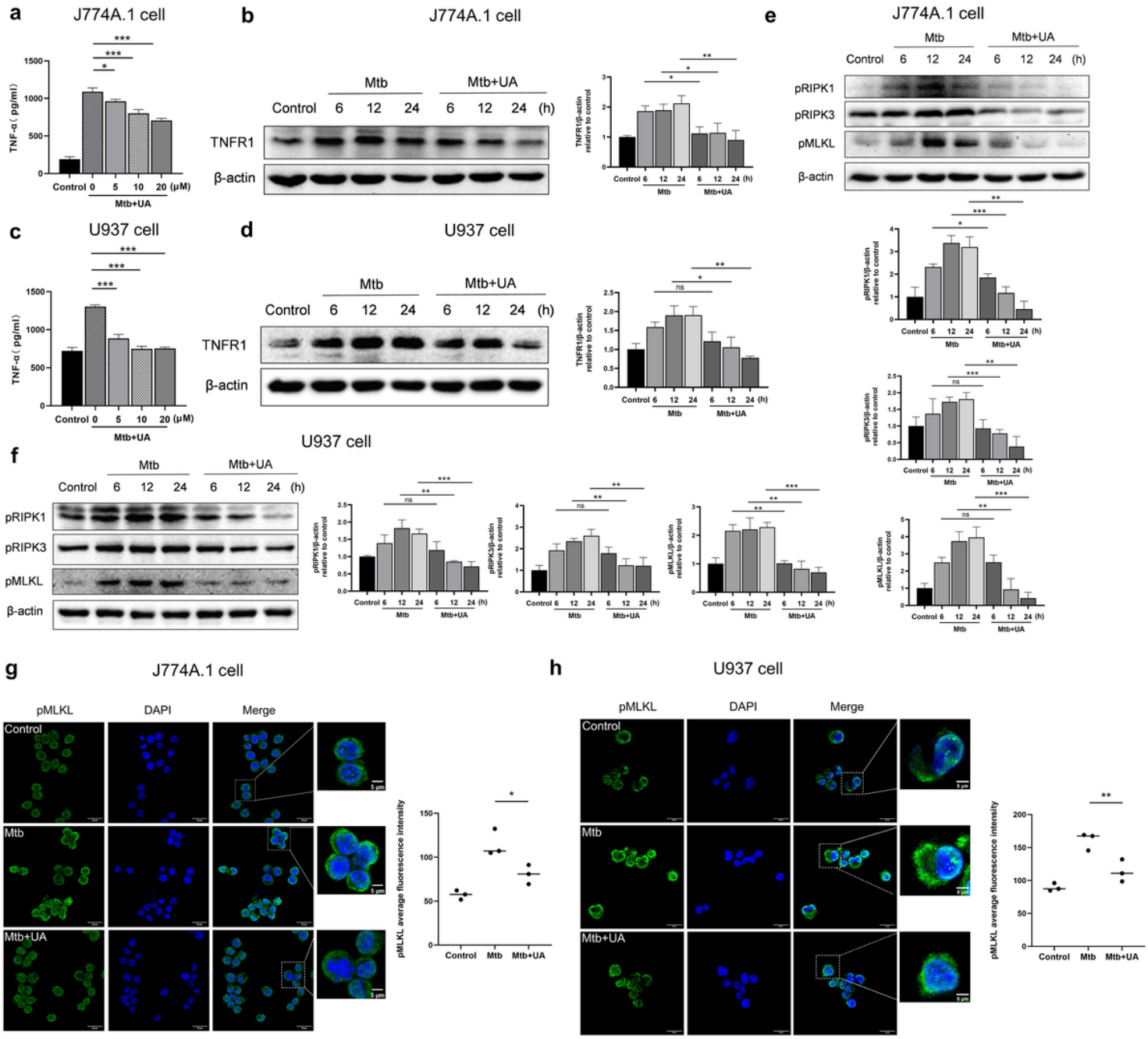

Figure 4

UA alleviates necroptosis in Mtb-infected macrophages. **a, c** Inhibition of Mtb-induced TNF-α release from J774A.1 and U937 cells at different concentrations of UA by ELISA. **b, d** Effect of UA on TNFR1 protein expression in J774A.1 and U937 cells by western blot. **e, f** The effects of UA on the expression of necroptosis key proteins phosphorylated RIPK1 (pRIPK1), phosphorylated RIPK3 (pRIPK3), and pMLKL in J774A.1 and U937 cells were determined by western blot assay. **g, h**Rabbit anti-pMLKL (green) and DAPI (blue) were used for immunofluorescence staining. The fluorescence signal and localization of pMLKL in J774A.1 and U937 cells were observed by confocal microscopy. Data are shown as mean ± SD of three independent experiments. ∗p < 0.05, ∗∗p < 0.01, and ∗∗∗p < 0.001. ns: nonsignificant.

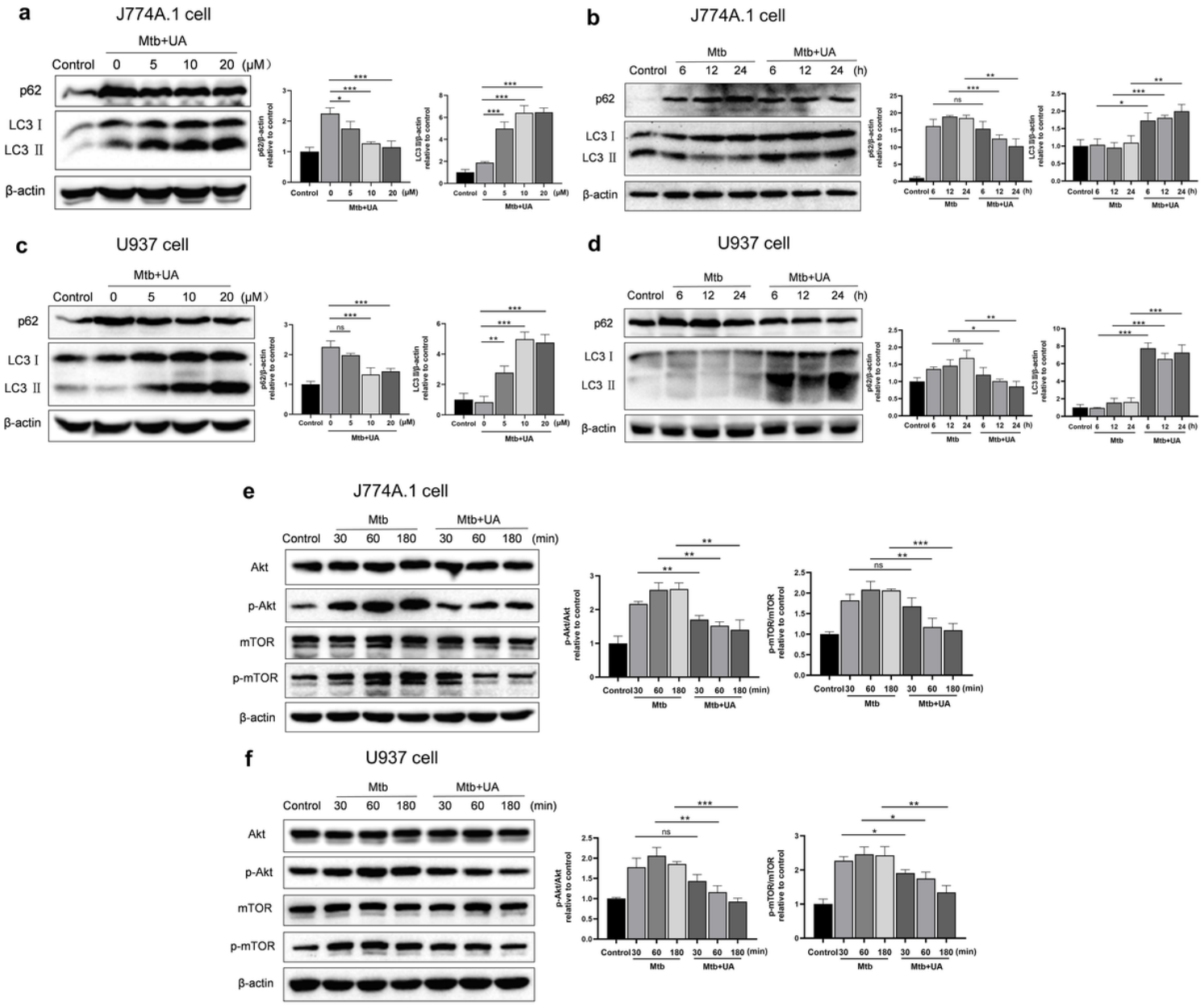

Figure 5

UA induces autophagy in macrophages by inhibiting the Akt/mTOR pathway. **a-d** In J774A.1 and U937 cells, the expression levels of p62 and LC3 II in cell lysates were determined by western blot assay, respectively. The bar graphs below show the statistical results of p62 and LC3 II protein levels. **e, f** Western blot assay of p-Akt and p-mTOR expression in J774A.1 and U937 cells. Total Akt and Total mTOR were used as internal controls, respectively. The bar chart below shows the statistical results of the relative intensity of p-Akt and p-mTOR. Data are shown as mean ± SD of three independent experiments. $*p < 0.05$, $**p < 0.01$, and $***p < 0.001$. ns: nonsignificant.

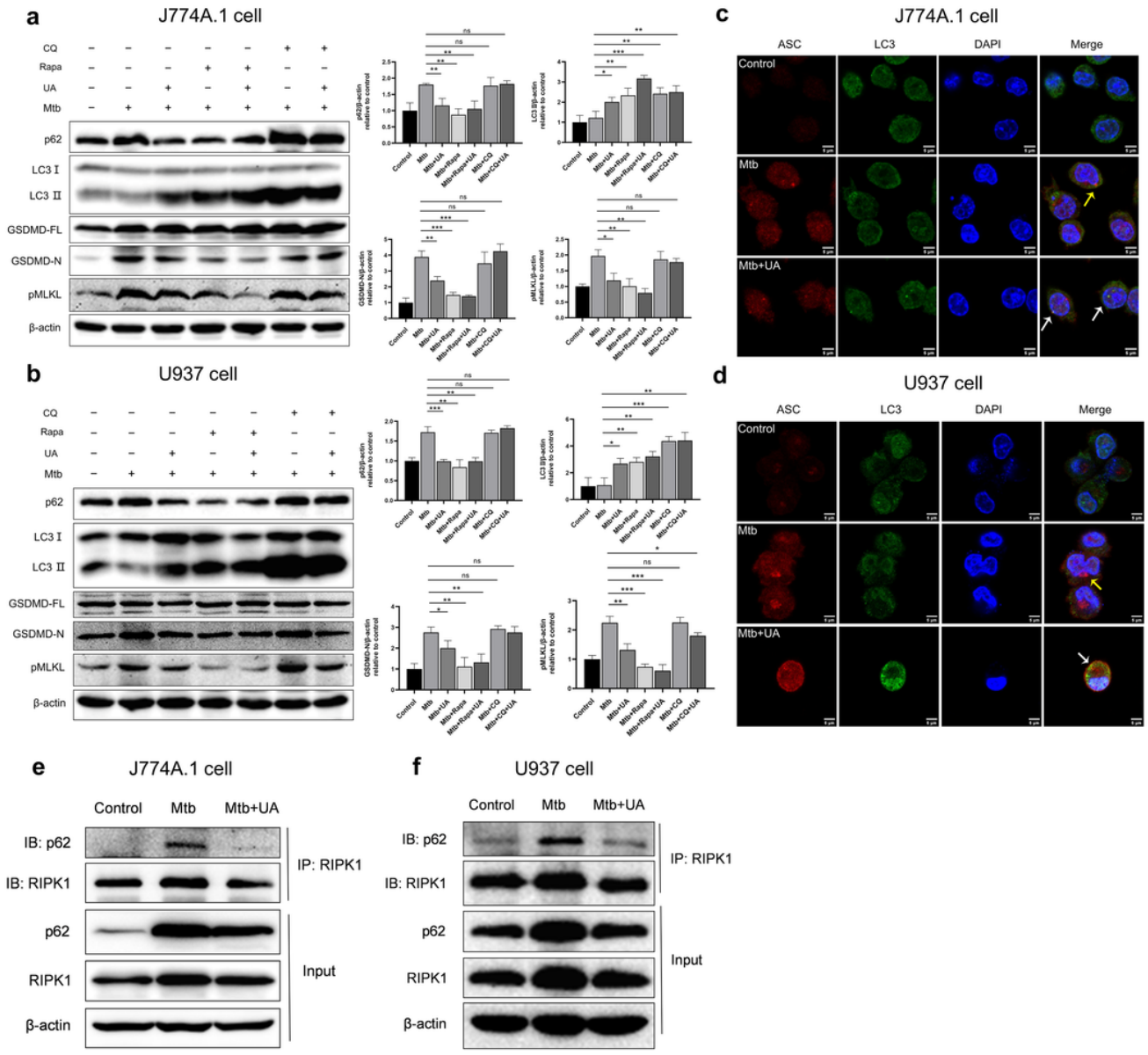

Figure 6

UA inhibits pyroptosis and necroptosis by promoting autophagy. **a, b** Detection of p62, LC3 II, GSDMD-N, and pMLKL protein expression levels after addition of Rapa (1 μg/ml) or CQ (20 μM) in J774A.1 and U937 cells. The bar graph below shows the statistical results of the grayscale values of each protein level. **c, d**Confocal microscopic observation of J774A.1 and U937 cells after different treatments with anti-ASC (red), LC3 (green) and DAPI (blue), respectively. Yellow arrows indicate ASC spots and white arrows indicate co-location of ASC and LC3. **e, f** The effect of UA on the interaction of RIPK1 and p62 proteins was examined by immunoprecipitation with anti-RIPK1 antibody in J774A.1 and U937 cells that have been validated to express RIPK1 and p62 after Mtb treatment alone or in combination with UA. Data are shown as mean ± SD of three independent experiments. $*p < 0.05$, $**p < 0.01$, and $***p < 0.001$. ns: nonsignificant.

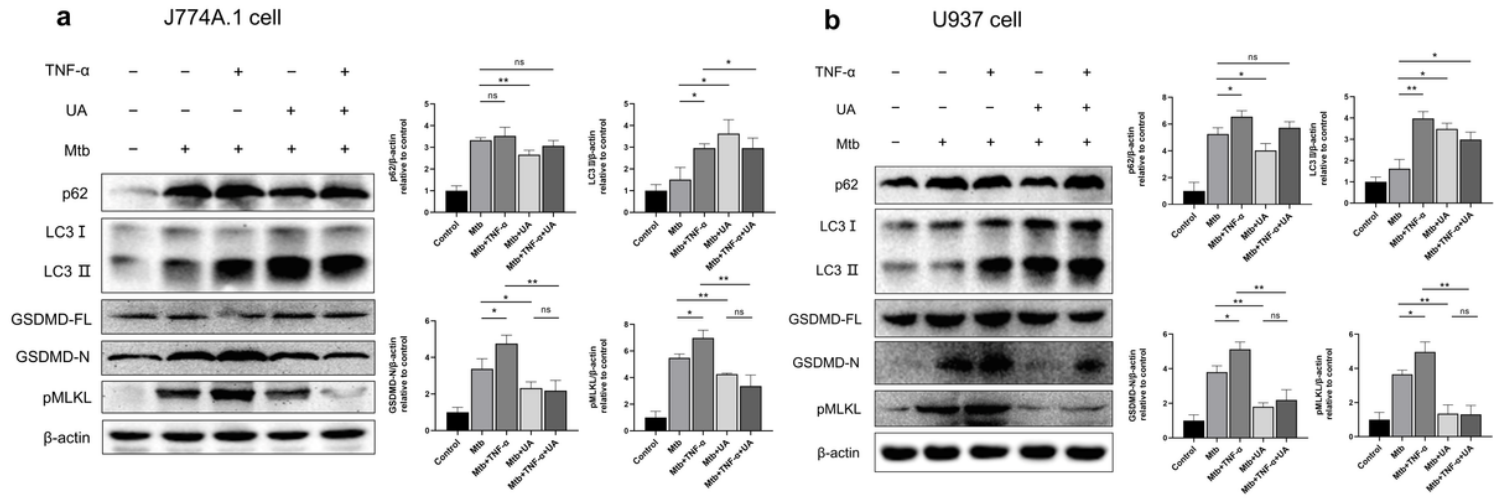

Figure 7

UA promotes autophagy and inhibits pyroptosis and necroptosis, which is related to TNF-α/TNFR1. **a, b** Western blot detection of pMLKL, GSDMD-N, p62 and LC3 II protein levels in lysates of Mtb-infected J774A.1 cells or U937 cells with or without TNF-α (30 ng/ml) or UA treatment. The bar chart below shows the statistical results of the grayscale values for each protein level. Data are shown as mean ± SD of three independent experiments. $*p < 0.05$, $**p < 0.01$, and $***p < 0.001$. ns: nonsignificant.

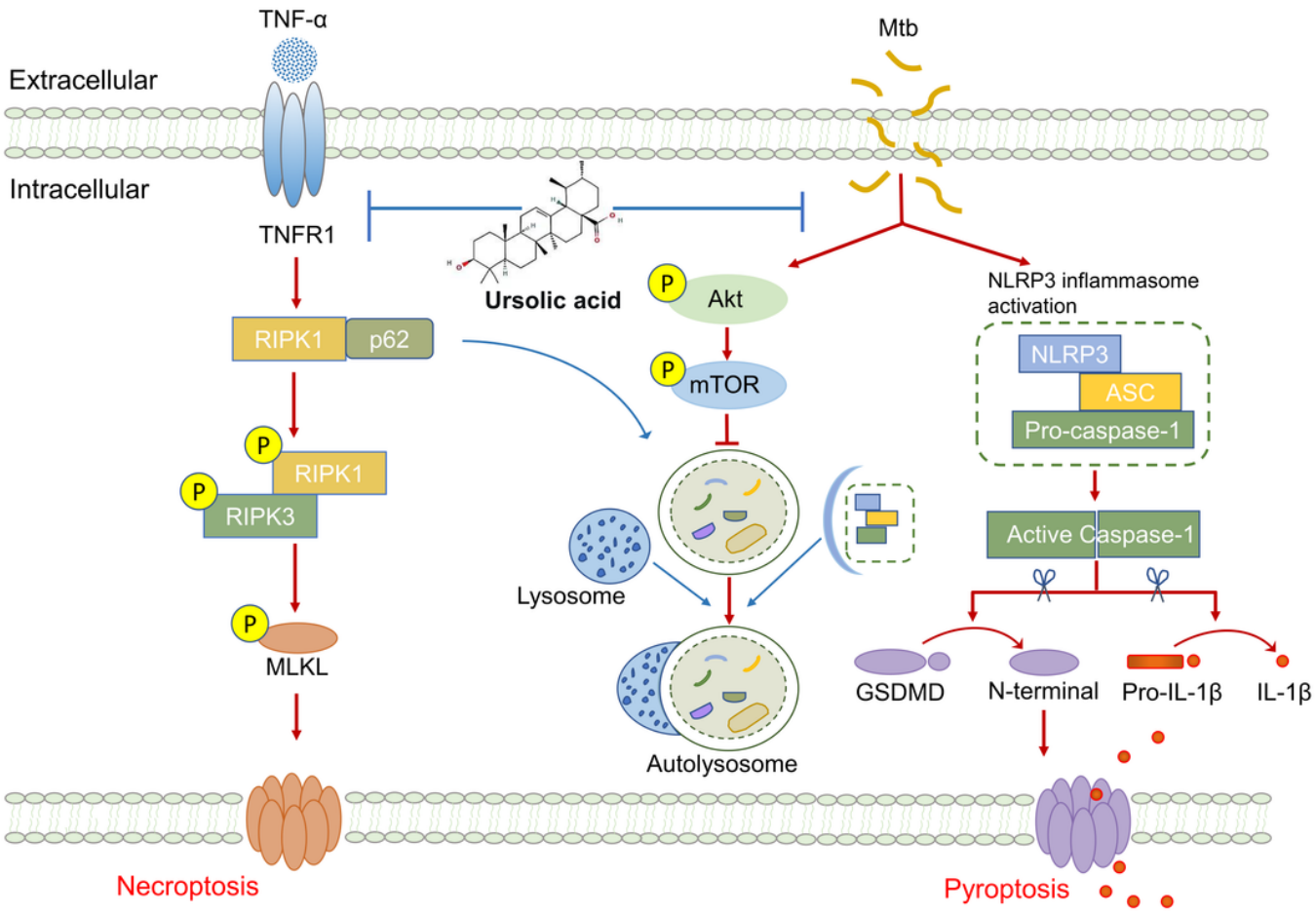

Figure 8

An illustration of the role of UA in inhibiting pyroptosis and necroptosis in Mtb-infected macrophages. In the present study, we found that UA promotes autophagy through synergistic inhibition of Akt/mTOR and TNF-α/TNFR1 signaling pathways, thereby inhibiting pyroptosis and necroptosis in Mtb-infected macrophages.